Green Chemistry

PAPER

View Article Online
View Journal

Cite this: DOI: 10.1039/d5gc05226b

Deep eutectic solvents as recyclable solvent–electrolyte systems for electroreductive C–O cleavage of lignin models

Astrid Kjær Steffensen, [a] Helena Lundberg *[b] and Anders Riisager *[a]

Received 2nd October 2025,
Accepted 30th March 2026

DOI: 10.1039/d5gc05226b

rsc.li/greenchem

Deep eutectic solvents (DESs), formed from hydrogen bonding acceptors and donors, are investigated as recyclable solvent–electrolyte systems for the electroreductive cleavage of C–O bonds in lignin model ethers. The widely used DES composed of choline chloride and methyl urea demonstrates a suitable electrochemical window and high cathodic stability enabling efficient cleavage of benzyl phenyl ether, achieving up to 97% selectivity for phenol over three reaction cycles in a simple, undivided cell without catalysts or additives. Optimization studies show that the choice of electrode material significantly affects both conversion and yield. Furthermore, the method is applicable to a selection of lignin model ethers, with observed reactivity trends correlating to the substrate structure and solubility. This work highlights the potential of low-cost DESs as novel, dual-function, and recyclable media for green electrosynthesis, providing a foundation for future advances in electrochemical lignin depolymerization. Notably, the approach reduces waste associated with traditional supporting electrolyte salts and solvents in electrosynthesis, and continued improvements in faradaic efficiency and process integration will unlock the full green potential of this novel strategy.

Green foundation

1. Deep eutectic solvents (DESs) are introduced as non-volatile, cheap solvent–electrolyte systems with the potential to solubilize biomass for reductive electrosynthesis. The use of DES systems is a promising approach for reducing waste formation in organic electrosynthesis, often generated from supporting electrolyte salts and organic solvents.
2. DESs are showcased as solvent–electrolyte systems for electroreductive C–O cleavage of various lignin model ether compounds, achieving up to 97% phenol selectivity. The DES is reusable in at least three consecutive reactions without a significant decrease in phenol selectivity.
3. Mass transfer in DES systems limits conversion and faradaic efficiency and future research should target improving the mass transfer for wider use of DESs as electrolyte systems. Furthermore, coupling reductive C–O cleavage with a productive counter reaction could increase the atom economy of the process allowing electroreductive biomass valorization as a next step.

Introduction

In electrochemical synthesis, electrons are used to activate molecules and drive redox reactions under ambient conditions, enabling the development of benign chemical production with minimized need for auxiliary reagents.[1,2] This approach can offer greater energy efficiency, improved selectivity, and higher atom economy compared to traditional synthetic methods, making electrosynthesis promising as a more sustainable alternative to conventional approaches.[3–6] However, electrosynthesis in organic solvents typically relies on supporting electrolytes, such as perchlorates or quaternary ammonium salts, to ensure sufficient electric conductivity. While these supporting electrolytes are generally non-reactive and redox stable species, their interactions with electrode surfaces, reactants, and intermediates can influence reaction outcomes.[7] Supporting electrolyte salts are often used in large excess and must be separated from the products after the reaction, leading to significant waste generation or downstream processing steps for their recovery that increases the complexity and costs of the synthetic process. The widespread use of organic solvents – often highly flammable and toxic – to dissolve large quantities of supporting electrolytes further limits the sustainability of organic electrosynthesis.[8,9]

A range of strategies has been developed to mitigate the drawbacks associated with supporting electrolytes in electrosynthesis, including *in situ* generation of electrolytes,[10,11]

[a]*Technical University of Denmark, Department of Chemistry, 2800 Kgs. Lyngby, Denmark. E-mail: ar@kemi.dtu.dk*
[b]*Department of Chemistry, KTH Royal Institute of Technology, S-100 44 Stockholm, Sweden. E-mail: hellundb@kth.se*

reduction of electrolyte concentration,[12] and the use of microflow cells with narrow inter-electrode gaps to maintain conductivity in the absence of electrolyte salts.[13,14] Another promising approach involves the design of electrolyte systems that allow for easy separation and reuse (Fig. 1A), such as solid bases (solid electrolytes)[15–17] and immobilized electrolytes on polymer backbones (polyelectrolytes).[18] While these methods facilitate straightforward separation *via* filtration, they still

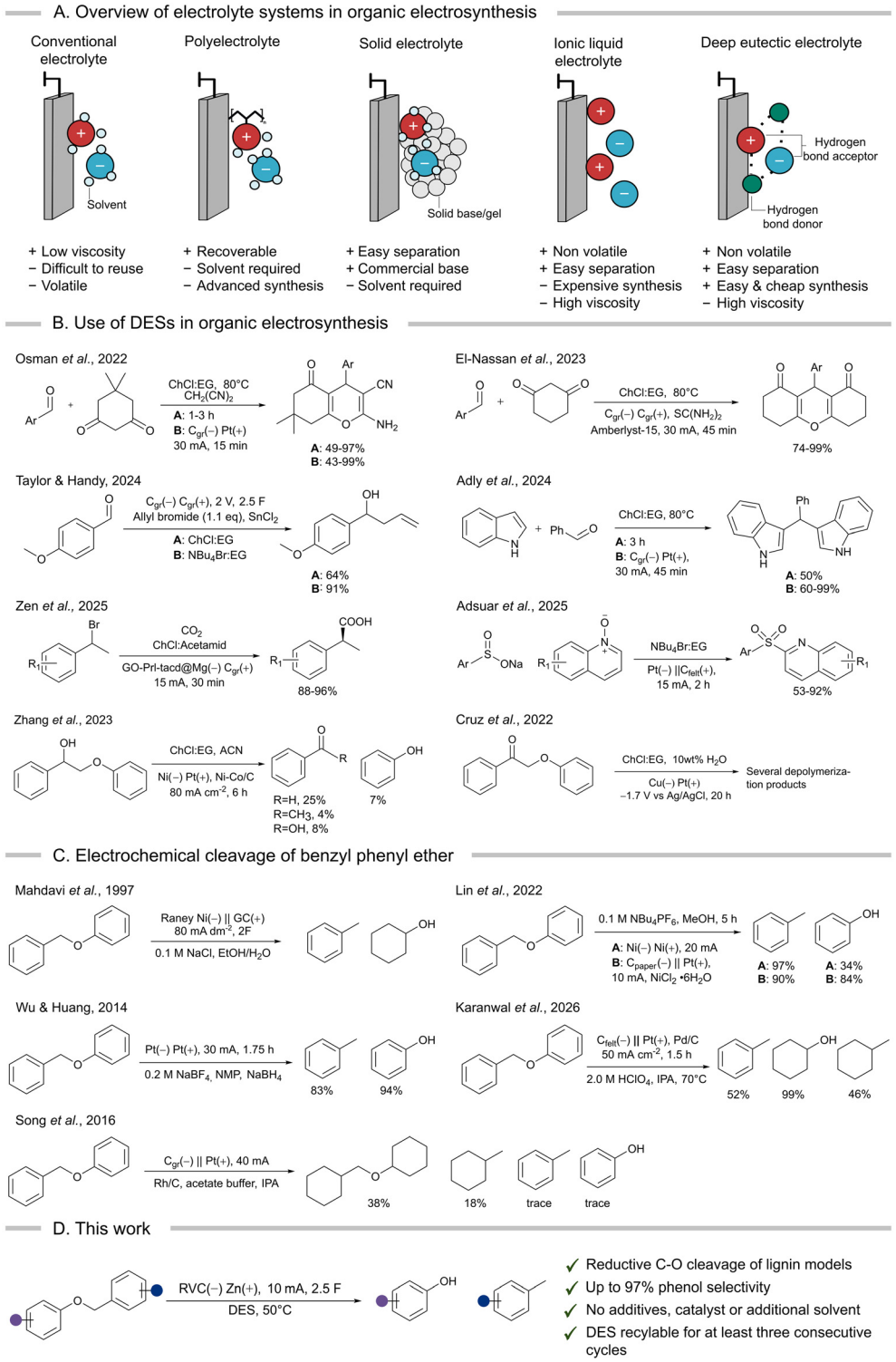

Fig. 1 DESs as recyclable electrolytes for C–O bond cleavage. (A) Approaches for recyclable electrolytes in electrosynthesis. (B) Use of DESs in electrosynthesis. (C) Electrochemical cleavage of benzyl phenyl ether (|| denotes a divided cell). (D) This work.

require a reaction solvent. In this context, alternative solvents capable of serving dual roles – as both solvent and electrolyte – are of particular interest, especially if they can be easily separated from the product and reused. Ionic liquids (ILs) exemplify such systems and have been applied in electrosynthesis for various transformations,[19] including carboxylation[20–22] and phosphorylation.[23] Nevertheless, the use of ILs in electrosynthesis is hampered by their relatively low conductivity and high cost.[19]

Deep eutectic solvents (DESs), formed by mixing a hydrogen bond acceptor (HBA) and a hydrogen bond donor (HBD) in a specific ratio to reach a eutectic point, share many properties with ILs but are significantly cheaper.[24,25] The high thermal stability, low volatility and immiscibility with organic solvents of DESs enable their recovery and recycling by various methods. These include practical methods such as liquid–liquid extraction, anti-solvent addition and short-path distillation,[26] rendering DESs promising as recyclable electrolyte/solvent systems. A distinct feature of DESs is their ability to solubilize biomass, making them highly attractive for biorefinery applications.[27,28] In the context of lignin, DESs can enable up to 50% (w/w) material dissolution, whereas in ILs, similar results require higher temperatures.[29–31] Lignin constitutes up to 30 wt% of lignocellulosic biomass, but remains underutilized in biorefinery applications, in contrast to the cellulose and hemicellulose fractions that have well-established industrial valorization pathways.[32] Electrochemical oxidative depolymerization of lignin into low-molecular-weight chemicals has been widely studied in aqueous electrolytes with various electrocatalysts.[33–37] In contrast, analogous reductive depolymerization of lignin is less explored, despite the potential advantages, such as the production of value-added aromatics with high energy density due to increased hydrogen content.[38] Reports on reductive approaches for cleavage of dimeric lignin model compounds include studies on diphenyl ethers[39–41] and β-O-4 models[42–48] in aqueous and organic electrolytes.

DESs have been studied as electrolytes in electrochemical applications, including battery chemistry[49,50] and electrodeposition;[51] however, their use in electrosynthesis remains limited (Fig. 1B). Transformations in neat DES systems include the electrochemically assisted formation of bis(indoyl)methane,[52] pyran,[53] and xanthene derivatives.[54] DES systems have also recently been successfully applied for electrochemical sulfonation,[55] allylation[56] and carboxylation.[57] Furthermore, oxidative electrochemical depolymerization of lignin has shown promise in DES–water mixtures[58,59] and emulsions,[60] yielding vanillin and guaiacol as the major products. On the other hand, the C–O cleavage of a β-O-4 lignin model, 2-phenoxyacetophenone, was studied by Cruz *et al.*[61] under reductive conditions in a DES–H_2O electrolyte. While selective β-O-4 cleavage was not observed, it was shown that the electrocatalytic hydrogenation generated different product types depending on the cell type. Likewise, Zhang *et al.* studied electrocatalytic cleavage of the β-O-4 lignin model 2-phenoxy-1-phenylethanol, utilizing a nickel–cobalt catalyst in a DES–acetonitrile electrolyte, which enabled both C–O and C–C cleavage.[62] Notably, DESs consisting of choline chloride and ethylene glycol have mostly been utilized, despite the large combinatorial space within the composition of DESs. Thus, their full potential as integrated solvent–electrolyte systems (deep eutectic electrolytes) for direct electrochemical transformations remains largely unexplored.

Herein, we focus on the use of deep eutectic electrolytes as a medium for electroreductive C–O bond cleavage of an α-O-4 type lignin motif, utilizing benzyl phenyl ether as a model compound. Electrochemical reductive C–O cleavage of benzyl phenyl ether has previously been studied in a range of conventional solvents (Fig. 1C). Using NaCl electrolyte in ethanol/water, Mahdavi *et al.* observed partial hydrogenation forming cyclohexane and toluene under reductive conditions.[63] Electrocatalytic hydrogenation of benzyl phenyl ether was also studied by Song *et al.* using a Rh/C catalyst in aqueous isopropanol, where hydrogenation of the aromatic ring was more prevalent than C–O cleavage.[64] Recently, Karanwal *et al.* have demonstrated efficient Pd-catalyzed hydrogenolysis using a perchloric acid electrolyte.[65] Selective reductive C–O cleavage of several lignin bond motifs was achieved by Wu and Huang, utilizing borohydride as a promoter in an NMP/$NaBF_4$ electrolyte system.[66] In this case, mechanistic studies show that both borohydride and the solvent act as proton sources for product formation. Lin *et al.* studied Ni-catalyzed C–O cleavage in methanol/NBu_4PF_6 electrolyte in both undivided and divided cells, showing that the phenol yield increased significantly by the use of a divided cell.[67] Furthermore, it was shown that Ni^0 played a central role in facilitating C–O cleavage.[68] Besides, in an attempt to utilize more environmentally friendly electrolytes, Zhang *et al.* recently demonstrated C–O cleavage of benzyl phenyl ether in methanol, yielding up to 95% benzaldehyde dimethyl acetal using $NaBF_4$ or NaCl as supporting electrolyte salts.[69,70]

In this work, we investigate a selection of DESs as a benign combined solvent–electrolyte system for the electroreductive cleavage of C–O bonds in lignin model compounds (Fig. 1D). A systematic study of benzyl phenyl ether **1a** with an α-O-4 type lignin motif reveals the effect that the DES composition, reaction temperature, and electrode materials have on the yield and selectivity of phenol (**2a**) as the target product. Among the tested systems, a DES composed of choline chloride and methyl urea enabled highly selective phenol formation without the need for catalysts or additives and using a simple undivided cell, achieving 97% selectivity after passing 2.5 F of charge. Importantly, the DES could be reused for at least three consecutive cycles without observable degradation, highlighting its potential to serve as a low-cost, robust, and sustainable medium for lignin electro-valorization.

Results and discussion

Electrochemical properties of DES systems

Six ammonium-based DESs (Table 1) were synthesized for their evaluation as electrolytes in reductive electrosynthesis (see the SI for details). Choline chloride with *N*-methyl urea

Table 1 Electrochemical properties of the synthesized DESs and a DMF/NBu_4PF_6 reference system

Entry	System	HBA : HBD (1 : 2 molar ratio)	Cathodic limit[a] (V *vs.* $Fc^{0/+}$)	Anodic limit[a] (V *vs.* $Fc^{0/+}$)	ECW (V)	Conductivity[d] (mS cm^{-1})
1	DES-1[b]	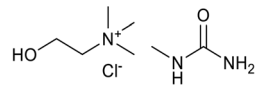	−3.34	0.88	4.22	2.1
2	DES-2	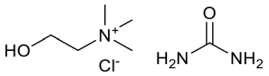	−3.36	1.13	4.49	2.6
3	DES-3	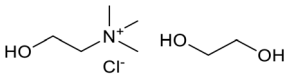	−3.03	0.60	3.63	16
4	DES-4	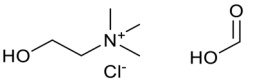	−2.63	0.67	3.30	30
5	DES-5	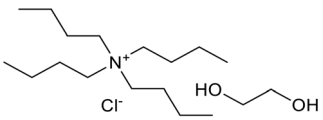	−3.45	0.69	4.14	1.9
6	DES-6[c]	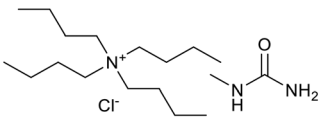	−3.23	0.63	3.86	—
7	DMF/0.1 M NBu_4PF_6	—	−3.45	1.29	4.74	6.3

[a] Limits determined for DESs by CV using a scan rate of 100 mV s^{-1} and a threshold current density of 0.5 mA cm^{-2} at room temperature with a glassy carbon (GC) disk working electrode, saturated calomel reference electrode (SCE), and Pt wire counter electrode (details in the SI, section 1.8). [b] CV measured at 30 °C. [c] CV measured at 80 °C. [d] Measured at 50 °C (details in the SI, section 1.9).

(DES-1) was selected due to its reported high cathodic stability,[71] and its well-established analogues choline chloride with urea (DES-2) and ethylene glycol (DES-3) were assessed for comparison. DES-4, based on choline chloride and formic acid, was selected to expand the scope of HBD's known to be beneficial in lignin applications.[72] To investigate the role of the HBA, analogues with tetrabutylammonium counterions were chosen (DES-5 and DES-6) as this cation is commonly used in conventional electrolyte systems for organic electrosynthesis. All synthesized DESs, except DES-6, were liquid at room temperature. Initially, the electrochemical redox potentials of the neat DESs were evaluated by cyclic voltammetry (CV) from which the anodic/cathodic limits and the electrochemical stability window (ECW) were determined (see the SI, Fig. S4–9).

As may be expected, the nature of the HBD and HBA greatly influenced the electrochemical stability windows (ECW) of the DESs (Table 1). For the choline chloride-based DESs (DES-1 to DES-4), the HBD significantly affected the cathodic limit that was found to increase in the order: formic acid (DES-4) < ethylene glycol (DES-3) < *N*-methyl urea (DES-1) ≈ urea (DES-2) with a difference of 730 mV between DES-2 and DES-4. This trend is consistent with previous reports and clearly demonstrates that the cathodic stability is correlated to the nature of the HBD.[71] The impact of the HBA for the ECW is less clear. When comparing DES-1 with DES-6 and DES-3 with DES-5 (Table 1, entries 1 *vs.* 6 and 3 *vs.* 5, respectively), the switch from choline chloride to tetrabutylammonium chloride as HBA resulted in a decrease of the anodic limit in the first case, while a slight increase was observed in the latter case. The same trend could be observed for the cathodic limit. The similar anodic limit of DES-3 to DES-6 could suggest that oxidation of chloride limits the anodic stability in these cases, whereas DES-1 and DES-2 exhibit considerably higher anodic limits. As such, interactions between the HBD and HBA affect the electrochemical properties of a DES and likely play a role in their degradation, although this is not well understood.[71] The combination of choline chloride and urea (DES-2) resulted in the largest ECW (4.49 V), while DES-5 showed the greatest cathodic stability, the latter being close to that of the conventional solvent/electrolyte system tetrabutylammonium hexafluorophosphate (NBu_4PF_6) in *N*,*N*-dimethylformamide (DMF) (Table 1, entry 5 *vs.* 7).

In addition to electrochemical stability, the conductivity is another important factor for electrolyte systems as it affects cell resistance and faradaic efficiencies of the electrochemical transformation.[73] As seen in Table 1, DES-1, DES-2 and DES-5 exhibit lower conductivities compared to the conventional electrolyte system (Table 1, entries 1, 2 and 5 *vs.* 7), whereas the less viscous DES-3 and DES-4 exhibit considerably higher values (Table 1, entries 3 and 4 *vs.* 7) (see the SI, Table S1 for viscosity data). It should be noted that the conductivity of the

conventional electrolyte is dependent on the concentration of supporting electrolyte salts and comparisons with the neat DES systems given in Table 1 should, thus, be made with caution.[74] In this case, the conductivity of the conventional electrolyte was measured at a 0.1 M concentration of supporting electrolyte.

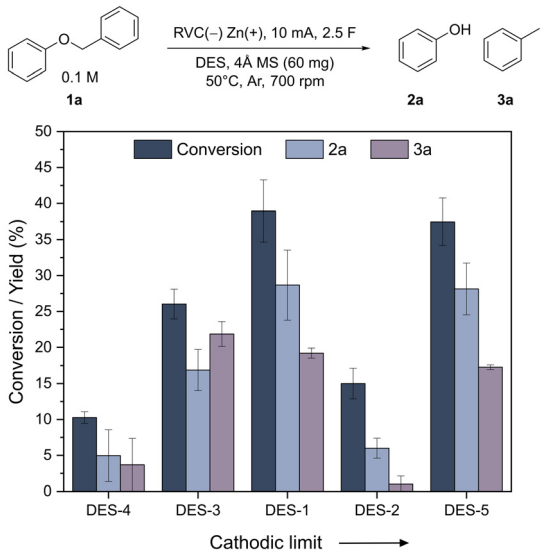

Fig. 2 Screening of different DESs as solvent–electrolyte systems for C–O cleavage of benzyl phenyl ether **1a**. Conversion and yields are determined by HPLC analysis (see the SI, section 1.6 for details).

Evaluation of DES systems for C–O cleavage

As several of the examined DESs exhibited high cathodic stability and sufficient conductivity (Table 1), all DESs that were liquid at room temperature (DES-1 to DES-5) were probed as electrolyte media for electroreductive C–O bond cleavage of the lignin model benzyl phenyl ether **1a** with an α-O-4 type lignin motif in an undivided cell under galvanostatic conditions (Fig. 2). Molecular sieves (4 Å MS) were added to absorb residual water and thus minimize the competing cathodic hydrogen evolution reaction (HER). Compared to organic solvents, DESs are more viscous (see the SI, Table S1) and a high surface area cathode material – reticular vitreous carbon (RVC) – was thus employed to facilitate mass transport (see the SI for details). The most effective electrolysis was achieved with DES-1 as the electrolyte medium (39% conversion and 29% yield of **2a**). As a general trend, the conversion and phenol yield correlate with the cathodic stability of the DES, with the notable exception of DES-2. Interestingly, DES-5 shows similar results to DES-1, although it was assessed to be more cathodically stable than DES-1 (Table 1). To probe the origin of this behavior, the reduction of **1a** was studied in the different DESs by means of CV (Fig. 3). This assessment revealed that the onset reduction potential for **1a** in DES-1, DES-3 and DES-5 was positively shifted compared to the value in a DMF electrolyte (−3.19 V). In contrast, DES-2 and DES-4 afforded no shift in the reductive onset potential of **1a**. This finding is consistent with the lower conversions and yields observed for reductive electrolysis of **1a** in the latter two DESs, indicating that both electrochemical stability of the electrolyte and its inter-

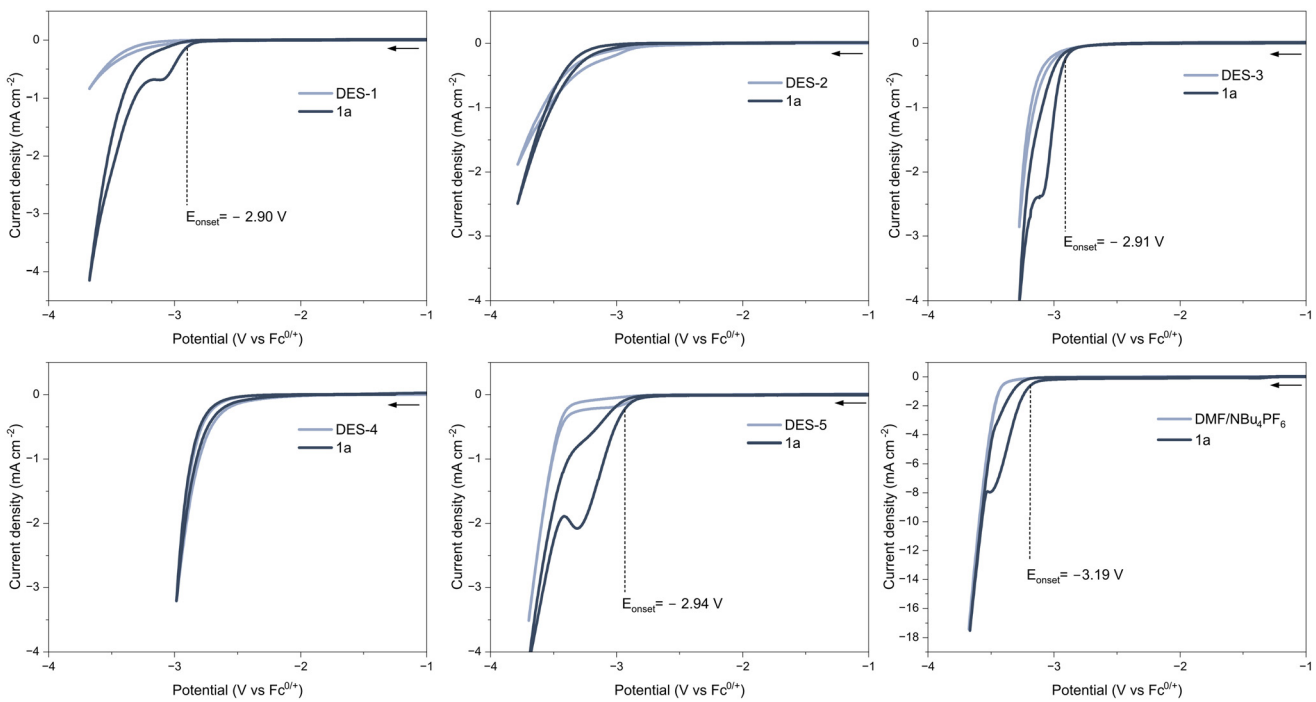

Fig. 3 CVs of benzyl phenyl ether **1a** (80 mM) in DESs and conventional electrolyte (DMF, 0.1 M NBu_4PF_6, 20 mM **1a**). Conditions: GC disk working electrode, SCE reference, and Pt wire counter electrode. The scan started at open circuit potential in a negative direction with a scan rate of 100 mV s^{-1}.

action with the organic substrate are of importance for the reaction outcome. The highest conversion of **1a** and the highest phenol yield (39% and 29%, respectively) were obtained in DES-1, in which the least negative onset potential of **1a** was observed. Such an anodic shift of the reduction potential is attractive as it enables the transformation to occur under milder conditions, suggesting that higher functional group tolerance and lower energy consumption may be possible.[75,76] Given the promising synthetic results combined with the moderate hygroscopic nature of DES-1 (see the SI, Table S1), this medium was chosen for the continued studies of electroreductive C–O bond cleavage.

Optimization and reuse of the DES-1 system for C–O cleavage

To further improve the conversion and product selectivity in the electroreduction of **1a** in DES-1, electrode materials and reaction conditions were screened (Table 2 and Fig. 4). To ensure adequate reproducibility, each reaction was repeated at least twice (see the SI, section 1.4 for details). Previous reports on the electrochemical C–O bond cleavage of **1a** in conventional solvent/electrolyte systems employed carbon-,[77] Pt-,[66] and Ni-based[67,68] cathodes (Fig. 1C). With the DES-1 system, all carbon-based cathodes (Table 2, entries 1–3) resulted in product formation, whereas Ni (Table 2, entry 4) and stainless steel (SS) (Table 2, entry 5) cathodes failed to convert **1a**. However, compared to the other carbon-based electrodes, the product selectivity was lower when using a graphite cathode (C_{gr}) (Table 2, entry 3 *vs.* 1 and 2) and the conversion was found to decrease upon reuse (see the SI, Table S3). This behavior occurred despite thorough electrode cleaning and polishing between reactions, possibly due to intercalation of ions in the graphite material. Likewise, a glassy carbon (GC) cathode (Table 2, entry 2) resulted in both lower substrate conversion and lower product selectivity compared to the use of a RVC cathode, as the higher surface area of the latter likely results in improved diffusion and thus a higher reaction rate.

To balance the net-cathodic transformation, the selection of the counter reaction is important to ensure efficient electrolysis.[78–81] Exchanging the sacrificial zinc anode with magnesium or aluminum electrodes (Table 2, entry 1 *vs.* 6 and 7) resulted in lower product yields and selectivity. This result may correlate with the increased resistance observed, causing the cell potential to exceed the capacity of the external power supply and thereby preventing the passing of 2.5 F of charge during the experiments (for details, see the SI, Fig. S2). The increased resistance may be understood in terms of anode passivation, as well as the lower solubility of Al^{3+} ions compared to Zn^{2+} ions in similar DESs.[82] The lower oxidation potential of Zn compared to Al and Mg[83] likely also contributes to higher product selectivity as oxidative side reactions may be more effectively suppressed. For reductive C–O bond activation, borohydride species have previously been demonstrated to act as anodic fuel,[81] as well as hydrogen donors.[66] However, the addition of borohydride to the DES electrolyte together with the use of a Zn anode resulted in lower product selectivity (Table 2, entry 8). Similarly, reduced phenol selectivity was observed when an inert carbon-based anode was used together with borohydride (see the SI, Table S3). In contrast, product selectivity was unaffected by the omission of molecular sieves (Table 2, entry 9), whereas the conversion of **1a** decreased, likely due to residual water leading to undesired hydrogen evolution. As expected, the reaction did not proceed in the absence of current (Table 2, entry 10). Notably, the results in Table 2 show that the yield of toluene was consistently lower compared to that of phenol. To probe if this observation was the result of a lack of H-donors in the system, additives such

Table 2 Optimization of C–O cleavage of benzyl phenyl ether **1a** in DES-1

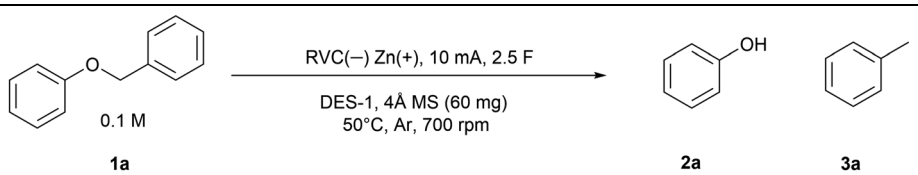

1a **2a** **3a**

		Yield (selectivity)[a] (%)		
Entry	Deviation	**2a**	**3a**	Conversion[a] (%)
1	None	29 (73)	19 (50)	39
2	GC cathode	14 (50)	5 (17)	27
3	C_{gr} cathode	6 (17)	6 (16)	35
4	Ni cathode	—	—	<5
5	SS cathode	—	—	<5
6	Mg anode[b]	3 (14)	2 (14)	19
7	Al anode[b]	10 (43)	10 (41)	24
8	NBu_4BH_4 (0.3 eq.)	28 (63)	14 (31)	44
9	No MS	25 (74)	16 (45)	34
10	No current	—	—	<5

[a] Conversions and product yields are determined by HPLC analysis (see the SI, section 1.6) and are the average of at least two identical experiments (see the SI, Table S3). [b] Resistance too high to pass 2.5 F (see details in the SI, Table S3 and Fig. S2). GC: glassy carbon, C_{gr}: graphite, MS: molecular sieves, RVC: reticular vitreous carbon, SS: stainless steel.

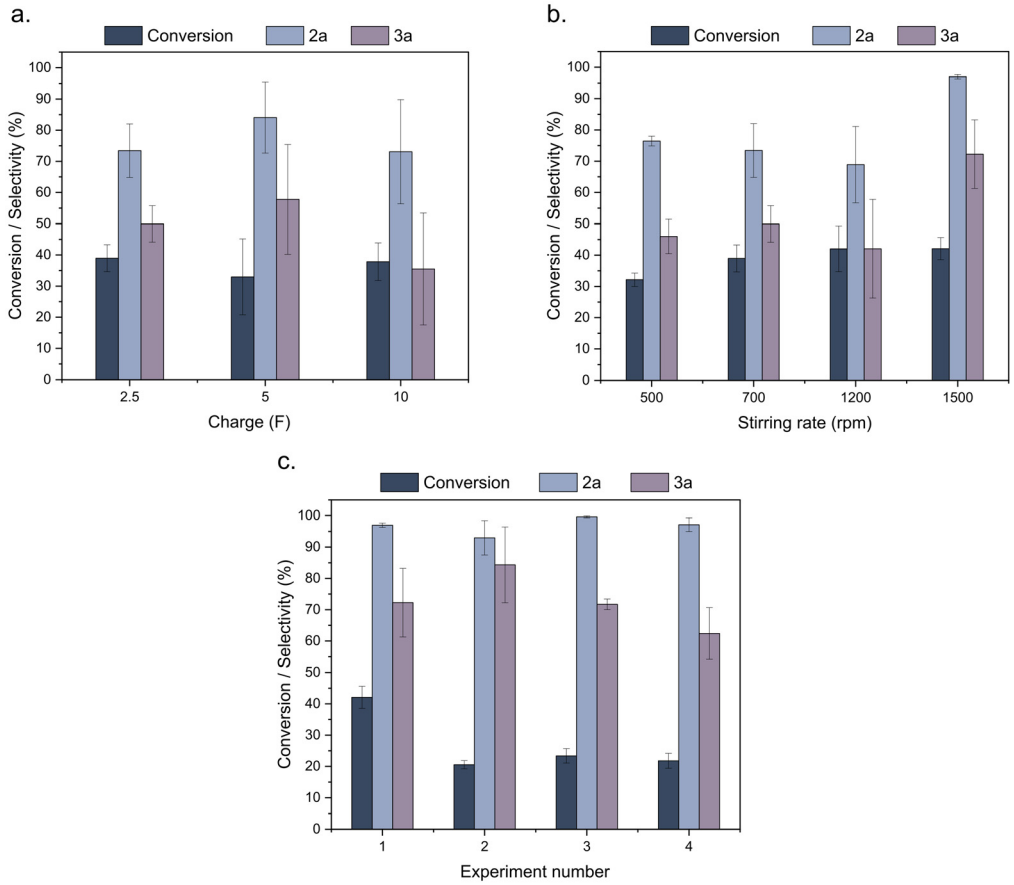

Fig. 4 Optimization and reuse of the DES-1 system for C–O cleavage of benzyl phenyl ether **1a**. (a) Effect of charge (2.5–10 F, 10 mA, 700 rpm). (b) Effect of stirring rate (500–1500 rpm, 10 mA, 2.5 F). (c) Recycling of DES-1 (2.5 F, 10 mA, 1500 rpm).

as $NaHCO_3$ and NBu_4PF_6 (see the SI, Table S3 for details) were assessed but did not improve the toluene yield. No benzylic coupling products, nor chlorinated or oxidized products, could be detected in the reaction mixture by HPLC (Fig. S23) or GC-MS (Fig. S41). Similarly, reduction products, such as cyclohexanol or 1-methylcyclohexane, could not be detected under these conditions by GC-MS. However, in addition to **1a**, **2a** and **3a**, GC-MS analysis showed trace amounts of 1-methylcyclohexa-1,4-diene, a Birch reduction product of toluene, which has previously been reported as a side-product for aryl ether cleavage.[66] These results suggest that the observed lower yield of toluene compared to phenol stems from a combination of continued reduction and higher volatility of the former, which may lead to an underestimation of the true yield.

Further optimization of the reaction parameters for the electroreduction of **1a** through a design of experiment (DoE) approach with temperature, current, and charge as factors indicated that temperature was a significant parameter for conversion and product yield (Table S4 and Fig. S3). Although the conductivity of DESs generally increases with temperature, higher reaction temperatures resulted in lower conversion and yield. Performing the reaction at lower temperatures of 30–40 °C proved unviable due to solidification of DES-1, which has a freezing point of 29 °C.[84] Additional experiments revealed that increasing the charge passed through the cell to 5 F increased product selectivity, whereas higher charges resulted in decreased selectivity, likely due to the onset of side-reactions (Fig. 4a). In contrast, the conversion of **1a** remained largely unaffected by increased charge, suggesting that mass transfer at the electrode surface may limit the overall conversion rate. This hypothesis was supported by observations indicating that an increase in stirring rate up to 1200 rpm resulted in higher conversion and product yields (Fig. 4b). A further increase in stirring rate to 1500 rpm had a marginal effect on conversion but appeared to positively influence the selectivity in product formation, resulting in a phenol selectivity of 97%. This increase in selectivity as a function of stirring rate may be attributed to a decreased thickness of the diffusion layer, resulting in improved transport of formed products away from the electrode.[85] Based on the high selectivity for **2a** achieved at 50 °C with a 1500 rpm stirring rate passing 2.5 F, these conditions were selected as optimal for subsequent experiments.

To evaluate the recyclability of DES-1, the solvent was collected after the electrochemical reaction and separated from the products by extraction before reuse in subsequent reactions (see the SI, section 1.5 for details). These recycling experiments demonstrated that DES-1 could be reused in at least three consecutive reactions without significant change in

Table 3 Electrochemical reductive C–O cleavage of lignin model ethers in DES-1

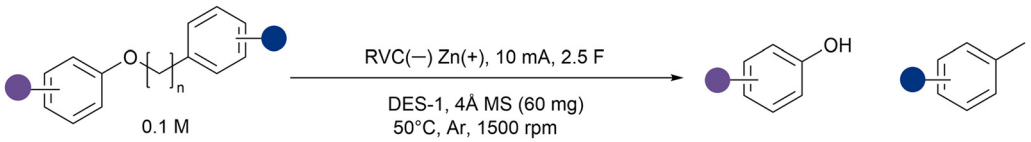

Entry	Substrate	Conversion (%)	Yield (selectivity)[a] (%)	
1	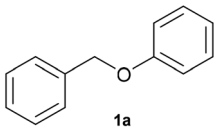 1a	42	 30 (72)	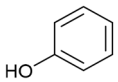 41 (97)
2	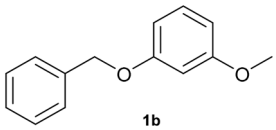 1b	25	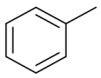 14 (53)	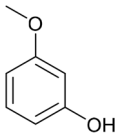 25 (97)
3	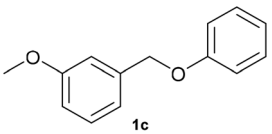 1c	31	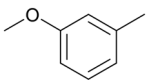 4 (13)	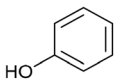 13 (43)
4	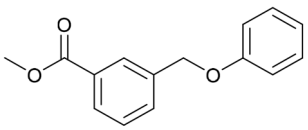 1d	57	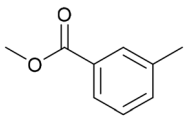 n.d.	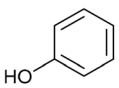 31 (55)
5	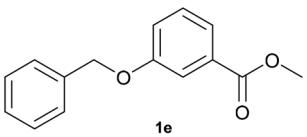 1e	—	—	—
6	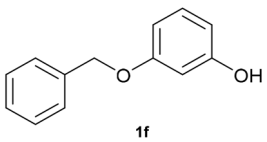 1f	43	 16 (37)	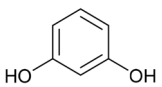 7 (16)
7	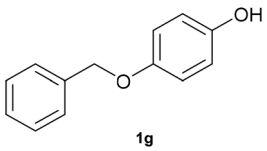 1g	25	 23 (92)	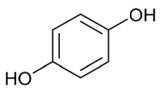 11 (44)
8	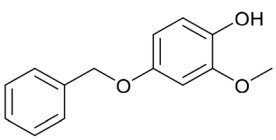 1h	27	 21 (78)	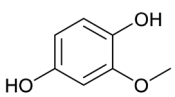 3 (12)
9	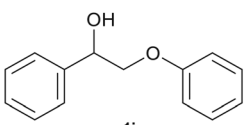 1i	16	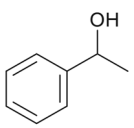 n.d.	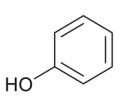 11 (67)

Table 3 *(Contd.)*

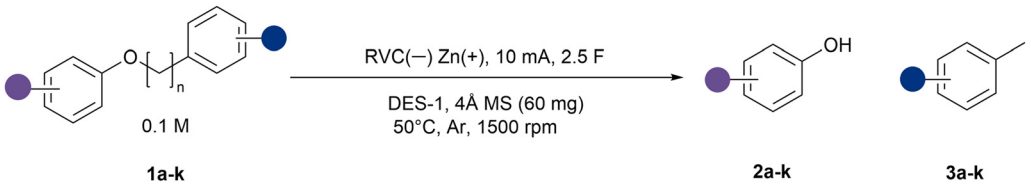

1a-k 2a-k 3a-k

Entry	Substrate	Conversion (%)	Yield (selectivity)[a] (%)	
10	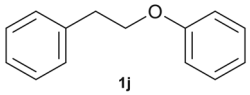 1j	—	—	—
11	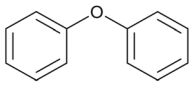 1k	24	 n.d.	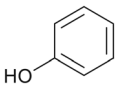 2 (10)

[a] Conversions and yields are determined by HPLC analysis (see the SI, section 1.6). n.d.: not detected.

phenol selectivity (Fig. 4c). However, a gradual decrease in the conversion of **1a** was observed upon recycling, likely due to the accumulation of residual water in the recycled DES – a factor that could not be fully mitigated by the addition of molecular sieves (see the SI, Table S2). Analysis of the recycled DES-1 by ^{1}H nuclear magnetic resonance (NMR) spectroscopy (see the SI, Fig. S34) showed no evidence of structural decomposition during electrolysis. Instead, ^{1}H-NMR analysis of the recycled DES showed changes in the chemical shifts that can be attributed to increased water content (Fig. S34 and S35).[86,87] While additional work is required for effective drying, these results suggest that DES-1 can be used as a recyclable electrolyte. With further optimization of the DES recovery method *via* the wide range of available routes, including distillation, extraction and anti-solvent addition, there is great potential for more sustainable and user-friendly reuse of this electrolyte system compared to what is possible for organic solvents with supporting electrolyte salts.

The use of a conventional electrolyte (DMF/NBu_4PF_6) instead of DES-1 under optimized conditions (1500 rpm, 2.5 F, RVC(−)Zn(+)) resulted in higher conversion of **1a** (71% *vs.* 42%), likely due to the lower viscosity of the former that leads to improved mass transport. Nevertheless, lower selectivities for phenol (69% *vs.* 97%) and toluene (57% *vs.* 72%) were observed in the conventional electrolyte compared to DES-1 (see the SI, Table S3 for details). This finding may potentially be attributed to DES stabilization of formed products *via* hydrogen bonding,[88] thereby preventing electrochemical degradation. Similarly, the use of DES-1 resulted in lower conversion rates compared to earlier reported protocols on reductive C–O cleavage of **1a** in conventional electrolyte (Fig. 1C), which all achieved near full conversion.[63–70] However, in terms of phenol selectivity, the current protocol achieves similar – or even higher – selectivity compared to these protocols without the use of catalysts, additives or divided cell configurations.

C–O cleavage of other lignin model ethers in the DES-1 system

With optimized conditions for the DES-1 system at hand, the reductive C–O bond cleavage for a selection of other lignin model ether compounds was examined (Table 3). For the methoxy derivative **1b** (Table 3, entry 2), a phenol selectivity identical to that of **1a** (Table 3, entry 1) was observed, while a considerably lower selectivity was observed for the isomer **1c** (Table 3, entry 3). Due to the similar reductive onset potential for **1b** and **1c** (Fig. S13 and S14), steric effects are likely the cause of these selectivity differences. The ester-substituted **1d** resulted in similar phenol selectivity to **1c** (Table 3, entry 4), whereas the isomeric **1e** (Table 3, entry 5) showed a low solubility in DES-1 and remained unconverted during electrolysis. With a hydroxy group at the *meta* position, **1f** resulted in lower selectivity for the phenolic product while the toluene selectivity was moderate (Table 3, entry 6). With the hydroxy group instead placed at the *para* position, **1g** resulted in high selectivity for toluene and moderate selectivity for the phenolic product (Table 3, entry 7). With the addition of a methoxy group at the *meta* position, **1h** resulted in similar conversion with overall lower product yields (Table 3, entry 8). The lower selectivity of the phenolic product in these cases compared to that of the benchmark substrate **1a** could be the result of faster product degradation of diphenols compared to phenol.[89] The C–O bond cleavage of the β-O-4 type model **1i** (Table 3, entry 9) exhibited good phenol selectivity (67%), albeit low conversion, under the applied conditions. Conversely, compound **1j** (Table 3, entry 10) did not convert under the applied conditions, likely due to its highly negative reduction potential that lies outside the ECW of DES-1 (see the SI, Fig. S21). For the same reason, the C–O bond cleavage of the diphenyl ether **1k** with a 4-O-5 type lignin motif was sluggish and unselective (Table 3, entry 11; see the SI, Fig. S22). Overall, reductive C–O bond cleavage of a range of lignin

model compounds showed promising results for α-O-4 cleavage, considering that the conditions were not optimized individually for every compound.

Conclusions

A series of DESs, composed of ammonium salts as hydrogen bond acceptors (HBAs) and diols or ureas as hydrogen bond donors (HBDs), was investigated as novel solvent–electrolyte systems for electroreductive C–O bond cleavage of lignin model ether compounds. Relying on its high cathodic stability, choline chloride–methyl urea (DES-1) was pertinent for electrochemical cleavage of phenyl ethers, enabling selectivities up to 97% towards phenol after optimization of various reaction parameters. Notably, this product selectivity was achieved without the use of additives or catalysts in a simple, undivided cell setup and DES-1 could successfully be reused with maintained product selectivity over three consecutive reaction cycles. Furthermore, the DES-1 electrolyte was successfully used for electroreductive C–O bond cleavage in a selection of lignin model compounds. While improvements of mass transfer, faradaic efficiencies and reduced water content in recycled DESs are challenges to address in future work, this study serves as a starting point for exploration of electroreductive transformations in DES media, including lignin depolymerization.

Author contributions

AKS: investigation, methodology, validation, visualization, and writing – original draft. HL: conceptualization, funding acquisition, supervision, and writing – review & editing. AR: project administration, conceptualization, funding acquisition, supervision, and writing – review & editing.

Conflicts of interest

There are no conflicts to declare.

Data availability

The data supporting this article have been included as part of the supplementary information (SI). See DOI: https://doi.org/10.1039/d5gc05226b

Acknowledgements

This work was financially supported by the Nordic Five Tech Alliance, the Swedish Foundation for Strategic Research (grant no. FFL21-0005), KTH Royal Institute of Technology, and the Technical University of Denmark. Assoc. Prof. Martin Nielsen and Prof. Kristoffer Almdal (Department of Chemistry, Technical University of Denmark) are gratefully acknowledged for providing access to a potentiostat and for their input on the rheology of fluids and access to a rheometer, respectively.

References

1 D. Pollok and S. R. Waldvogel, *Chem. Sci.*, 2020, **11**, 12386–12400.
2 P. Röse, P. Neugebauer, S. Tamang, S. R. Waldvogel and U. Krewer, *Chem. Ing. Tech.*, 2025, **97**, 395–410.
3 Y. H. Budnikova, E. L. Dolengovski, M. V. Tarasov and T. V. Gryaznova, *J. Solid State Electrochem.*, 2024, **28**, 659–676.
4 S. Cembellín and B. Batanero, *Chem. Rec.*, 2021, **21**, 2453–2471.
5 J. Seidler, J. Strugatchi, T. Gärtner and S. R. Waldvogel, *MRS Energy Sustain*, 2020, **7**, 42.
6 Y. Yuan and A. Lei, *Nat. Commun.*, 2020, **11**, 802.
7 L. G. Gombos, J. Nikl and S. R. Waldvogel, *ChemElectroChem*, 2024, **11**, e202300730.
8 R. Francke, *Curr. Opin. Electrochem.*, 2022, **36**, 101111.
9 J. M. Ramos-Villaseñor, F. Sartillo-Piscil and B. A. Frontana-Uribe, *Curr. Opin. Electrochem.*, 2024, **45**, 101467.
10 A. A. Al-Romema, H. Xia, K. J. J. Mayrhofer, S. B. Tsogoeva and P. Nikolaienko, *Chem. – Eur. J.*, 2024, **30**, e202402696.
11 F. A. Breitschaft, A. L. Saak, C. Krumbiegel, A. d. A. Bartolomeu, T. Weyhermüller and S. R. Waldvogel, *Org. Lett.*, 2025, **27**, 1210–1215.
12 D. S. P. Cardoso, B. Šljukić, D. M. F. Santos and C. A. C. Sequeira, *Org. Process Res. Dev.*, 2017, **21**, 1213–1226.
13 A. A. Folgueiras-Amador, X. Y. Qian, H. C. Xu and T. Wirth, *Chem. – Eur. J.*, 2018, **24**, 487–491.
14 N. Tanbouza, T. Ollevier and K. Lam, *iScience*, 2020, **23**, 101720.
15 T. Tajima, H. Kurihara and T. Fuchigami, *J. Am. Chem. Soc.*, 2007, **129**, 6680–6681.
16 F. Ferlin, F. Valentini, F. Campana and L. Vaccaro, *Green Chem.*, 2024, **26**, 6625–6663.
17 T. Tajima, S. Ishino and H. Kurihara, *Chem. Lett.*, 2008, **37**, 1036–1037.
18 B. Schille, N. O. Giltzau and R. Francke, *Angew. Chem., Int. Ed.*, 2018, **57**, 422–426.
19 M. Kathiresan and D. Velayutham, *Chem. Commun.*, 2015, **51**, 17499.
20 S. Mena and G. Guirado, *C – J. Carbon Res.*, 2020, **6**, 34.
21 S. Mena, J. Sanchez and G. Guirado, *RSC Adv.*, 2019, **9**, 15115.
22 S. Mena, S. Santiago, I. Gallardo and G. Guirado, *Chemosphere*, 2020, **245**, 125557.
23 X. Dong, R. Wang, W. Jin and C. Liu, *Org. Lett.*, 2020, **22**, 3062–3066.
24 J. Płotka-Wasylka, M. De La Guardia, V. Andruch and M. Vilková, *Microchem. J.*, 2020, **159**, 105539.
25 B. B. Hansen, S. Spittle, B. Chen, D. Poe, Y. Zhang, J. M. Klein, A. Horton, L. Adhikari, T. Zelovich,

B. W. Doherty, B. Gurkan, E. J. Maginn, A. Ragauskas, M. Dadmun, T. A. Zawodzinski, G. A. Baker, M. E. Tuckerman, R. F. Savinell and J. R. Sangoro, *Chem. Rev.*, 2021, **121**, 1232–1285.
26 A. Isci and M. Kaltschmitt, *Biomass Convers. Biorefin.*, 2021, **12**, 197–226.
27 H. Zhu, X. He, Z. Xu and L. Dai, *Green Chem.*, 2025, **27**, 1278–1299.
28 P. Verdía Barbará, H. Choudhary, P. S. Nakasu, A. Al-Ghatta, Y. Han, C. Hopson, R. I. Aravena, D. K. Mishra, A. Ovejero-Pérez, B. A. Simmons and J. P. Hallett, *Chem. Rev.*, 2025, **125**, 5461–5583.
29 T. Rashid, F. Sher, T. Rasheed, F. Zafar, S. Zhang and T. Murugesan, *J. Mol. Liq.*, 2021, **321**, 114577.
30 H. Malaeke, M. R. Housaindokht, H. Monhemi and M. Izadyar, *J. Mol. Liq.*, 2018, **263**, 193–199.
31 E. Melro, L. Alves, F. E. Antunes and B. Medronho, *J. Mol. Liq.*, 2018, **265**, 578–584.
32 K. Singh, S. Mehra and A. Kumar, *Green Chem.*, 2024, **26**, 1062–1091.
33 D. Gao, D. Ouyang and X. Zhao, *Green Chem.*, 2022, **24**, 8585–8605.
34 B. Ngokpho, P. Therdkatanyuphong, P. Krukkratoke, T. Khotavivattana, A. Boontawan and K. Ngamchuea, *RSC Adv.*, 2025, **15**, 33209–33223.
35 M. Zirbes, L. L. Quadri, M. Breiner, A. Stenglein, A. Bomm, W. Schade and S. R. Waldvogel, *ACS Sustainable Chem. Eng.*, 2020, **8**, 7300–7307.
36 N. Di Fidio, J. W. Timmermans, C. Antonetti, A. M. Raspolli Galletti, R. J. A. Gosselink, R. J. M. Bisselink and T. M. Slaghek, *New J. Chem.*, 2021, **45**, 9647–9657.
37 M. Breiner, M. Zirbes and S. R. Waldvogel, *Green Chem.*, 2021, **23**, 6449–6455.
38 X. Du, H. Zhang, K. P. Sullivan, P. Gogoi and Y. Deng, *ChemSusChem*, 2020, **13**, 4318–4343.
39 R. I. Pacut and E. Kariv-Miller, *J. Org. Chem.*, 1986, **51**, 3468–3470.
40 P. Dabo, A. Cyr, J. Lessard, L. Brossard and H. Ménard, *Can. J. Chem.*, 2011, **77**, 1225–1229.
41 M. Garedew, D. Young-Farhat, S. Bhatia, P. Hao, J. E. Jackson and C. M. Saffron, *Sustainable Energy Fuels*, 2020, **4**, 1340–1350.
42 A. Cyr, F. Chiltz, P. Jeanson, A. Martel, L. Brossard, J. Lessard and H. Ménard, *Can. J. Chem.*, 2000, **78**, 307–315.
43 Z. Fang, M. G. Flynn, J. E. Jackson and E. L. Hegg, *Green Chem.*, 2021, **23**, 412–421.
44 C. Yang, G. Magallanes, S. Maldonado and C. R. J. Stephenson, *J. Org. Chem.*, 2021, **86**, 15927–15934.
45 Y. He, X. Zeng, Z. Lu, S. Mo, Q. An, Q. Liu, Y. Yang, W. Lan, S. Wang and Y. Zou, *J. Am. Chem. Soc.*, 2024, **146**, 32022–32031.
46 Z. Yu, Z. Huang, L. Jiang and W. Li, *Chem. Commun.*, 2025, **61**, 2985–2988.
47 Z. Huang, Z. Yu, Z. Guo, P. Shi, J. Hu, H. Deng and Z. Huang, *Angew. Chem., Int. Ed.*, 2024, **63**, e202407750.
48 Z. Zhai, Y. Lu, L. Ouyang, J. Lu, W. L. Ding, B. Cao, Y. Wang, F. Huo, Q. Zhao, W. Wang, S. Zhang and H. He, *Nat. Commun.*, 2025, **16**, 3414.
49 M. K. Tran, M. T. F. Rodrigues, K. Kato, G. Babu and P. M. Ajayan, *Nat. Energy*, 2019, **4**, 339–345.
50 J. Yan, X. Zhao, J. Feng, Z. Li, Z. Bai, X. Hou, H. Li, H. Wei and S. Dou, *Angew. Chem., Int. Ed.*, 2025, **65**, e14392.
51 A. P. Abbott, *Curr. Opin. Green Sustainable Chem.*, 2022, **36**, 100649.
52 M. E. Adly, A. M. Mahmoud and H. B. El-Nassan, *BMC Chem.*, 2024, **18**, 139.
53 E. O. Osman, A. M. Mahmoud, S. S. El-Mosallamy and H. B. El-Nassan, *J. Electroanal. Chem.*, 2022, **920**, 116629.
54 H. B. El-Nassan, S. S. El-Mosallamy and A. M. Mahmoud, *Sustainable Chem. Pharm.*, 2023, **35**, 101207.
55 D. Adsuar, X. Marset, D. J. Ramón and N. Guijarro, *ChemSusChem*, 2025, **18**, e202501779.
56 S. Taylor and S. T. Handy, *Beilstein J. Org. Chem.*, 2024, **20**, 2217–2224.
57 A. A. Zen, Z. A. I. Alaridhee, R. Kamal Jameel, M. S. Mahdi, A. Salah Mansoor, U. K. Radi, A. H. Idan, H. Bahai, E. Berdimurodov, I. Eliboev and A. A. Almehizia, *Catal. Sci. Technol.*, 2025, **15**, 1185–1202.
58 E. Ceylan, B. Gürler-Akyüz, R. Kurt, A. Gencer, M. Akyüz and A. Kilic-Pekgözlü, *Wood Sci. Technol.*, 2024, **58**, 1645–1662.
59 D. Di Marino, D. Stöckmann, S. Kriescher, S. Stiefel and M. Wessling, *Green Chem.*, 2016, **18**, 6021–6028.
60 D. Di Marino, V. Aniko, A. Stocco, S. Kriescher and M. Wessling, *Green Chem.*, 2017, **19**, 4778–4784.
61 M. G. A. da Cruz, B. V. M. Rodrigues, A. Ristic, S. Budnyk, S. Das and A. Slabon, *Green Chem. Lett. Rev.*, 2022, **15**, 151–159.
62 J. Zhang, C. Suo, J. Sun, W. Li, S. Luo, C. Ma and S. Liu, *J. Electroanal. Chem.*, 2023, **938**, 117385.
63 B. Mahdavi, A. Lafrance, A. Martel, J. Lessard, H. Ménard and L. Brossard, *J. Appl. Electrochem.*, 1997, **27**, 605–611.
64 Y. Song, S. H. Chia, U. Sanyal, O. Y. Gutiérrez and J. A. Lercher, *J. Catal.*, 2016, **344**, 263–272.
65 N. Karanwal, S. Kim, Y. Liyanage, D. K. Lee and J. Kim, *Appl. Catal., B*, 2026, **381**, 125851.
66 W.-B. Wu and J. M. Huang, *J. Org. Chem.*, 2014, **79**, 10189–10195.
67 F. Lin, H. Y. Tse, H. C. Erythropel, P. V. Petrović, M. Garedew, J. Chen, J. C. H. Lam and P. T. Anastas, *Green Chem.*, 2022, **24**, 6295–6305.
68 F. Lin, P. V. Petrović, H.-Y. Tse, H. C. Erythropel, J. C.-H. Lam and P. T. Anastas, *Green Chem.*, 2023, **25**, 9720–9732.
69 H. Zhang, Z. Li, S. Tang, X. Yang, M. Li, J. Yang and L. Wei, *Ind. Crops Prod.*, 2024, **220**, 119292.
70 H. Zhang, Z. Li, X. Yang, M. Li, L. Wei and J. Yang, *Int. J. Biol. Macromol.*, 2024, **279**, 135260.
71 Q. Li, J. Jiang, G. Li, W. Zhao, X. Zhao and T. Mu, *Sci. China: Chem.*, 2016, **59**, 571–577.
72 Y. Oh, S. Park, D. Jung, K. K. Oh and S. H. Lee, *Int. J. Biol. Macromol.*, 2020, **165**, 187–197.
73 C. Stang and F. Harnisch, *ChemSusChem*, 2016, **9**, 50–60.

74 N. Shida, H. Takenaka, A. Gotou, T. Isogai, A. Yamauchi, Y. Kishikawa, Y. Nagata, I. Tomita, T. Fuchigami and S. Inagi, *J. Org. Chem.*, 2021, **86**, 16128–16133.
75 A. J. Bard and L. R. Faulkner, *Electrochemical Methods: Fundamentals and Applications*, John Wiley & Sons, Inc., 2nd edn, 2001.
76 F. Wang and S. S. Stahl, *Acc. Chem. Res.*, 2020, **53**, 561–574.
77 Y. Song, S. H. Chia, U. Sanyal, O. Y. Gutiérrez and J. A. Lercher, *J. Catal.*, 2016, **344**, 263–272.
78 S. D. Ware, W. Zhang, W. Guan, S. Lin and K. A. See, *Chem. Sci.*, 2024, **15**, 5814–5831.
79 Y. Li, L. Wen and W. Guo, *Chem. Soc. Rev.*, 2023, **52**, 1168–1188.
80 M. E. Avanthay, O. H. Goodrich, D. Tiemessen, C. M. Alder, M. W. George and A. J. J. Lennox, *JACS Au*, 2024, **4**, 2220–2227.
81 J. Kuzmin, M. Lill, G. Ahumada, E. Goossens, A. Kjær Steffensen, A. Riisager and H. Lundberg, *Angew. Chem., Int. Ed.*, 2025, **64**, e202501653.
82 A. P. Abbott, G. Capper, D. L. Davies, R. K. Rasheed and P. Shikotra, *Inorg. Chem.*, 2005, **44**, 6497–6499.
83 M. Klein and S. R. Waldvogel, *Angew. Chem., Int. Ed.*, 2022, **61**, e202204140.
84 A. P. Abbott, G. Capper, D. L. Davies, R. K. Rasheed and V. Tambyrajah, *Chem. Commun.*, 2003, **1**, 70–71.
85 C. Costentin and J. M. Savéant, *Proc. Natl. Acad. Sci. U. S. A.*, 2019, **166**, 11147–11152.
86 I. Delso, C. Lafuente, J. Muñoz-Embid and M. Artal, *J. Mol. Liq.*, 2019, **290**, 111236.
87 A. S. D. Ferreira, R. Craveiro, A. R. Duarte, S. Barreiros, E. J. Cabrita and A. Paiva, *J. Mol. Liq.*, 2021, **342**, 117463.
88 J. B. Barbieri, C. Goltz, F. Batistão Cavalheiro, A. Theodoro Toci, L. Igarashi-Mafra and M. R. Mafra, *Ind. Crops Prod.*, 2020, **144**, 112049.
89 A. S. Pavitt, E. J. Bylaska and P. G. Tratnyek, *Environ. Sci.: Processes Impacts*, 2017, **19**, 339–349.